SPANDIDOS PUBLICATIONS

MOLECULAR MEDICINE REPORTS 19: 1571-1580, 2019

Identification of differentially expressed genes in MG63 osteosarcoma cells with drug-resistance by microarray analysis

RUI CHEN[1], LI-HONG HUANG[2], YI-YAO GAO[3], JIAN-ZENG YANG[4] and YAN WANG[3]

[1]Department of Nuclear Medicine; Changhai Hospital of Shanghai, Shanghai 200433; [2]Geriatric Department; [3]Science Research Center, China-Japan Union Hospital of Jilin University, Changchun, Jilin 130033; [4]Henan Medical Key Laboratory of Molecular Imaging, Nuclear Medicine Department, The First Affiliated Hospital of Zhengzhou University, Zhengzhou, Henan 450000, P.R. China

Received March 26, 2018; Accepted November 9, 2018

DOI: 10.3892/mmr.2018.9774

Abstract. Osteosarcoma is the most common type of primary malignant bone tumor, with extremely poor prognosis in patients with metastatic disease and resistance to therapy, such as multidrug regimens. The mechanisms of drug resistance are quite complex and have not been fully elucidated; thus, novel therapeutic targets should be identified to alleviate drug resistance in osteosarcoma. In the present study, the transcriptomes of the human osteosarcoma cell line MG63 and vincristine (VCR)-resistant MG63 cells were compared by microarray analysis. A total of 1,300 genes (602 upregulated and 698 downregulated) were reported to be differentially expressed in MG63/VCR compared with MG63 cells. Bioinformatics analysis predicted that the differentially expressed genes were mainly enriched in the B cell receptor, UVA-induced mitogen-activated protein kinases and receptor tyrosine kinase 2/3 signaling pathways. In the present study, 10 of the dysregulated genes, including roundabout homolog 1, death-associated protein kinase 1 and A-kinase anchor protein 12 were further evaluated by reverse transcription-quantitative polymerase chain reaction. These results may aid the validation of candidate biomarkers for the treatment and prognosis of osteosarcoma, and provide novel insight into the molecular mechanisms underlying the drug resistance of osteosarcoma cells.

Introduction

Osteosarcoma is the most common type of primary malignant bone tumor with a high rate of metastasis (1). Furthermore, few biomarkers have been reported for early detection and differential diagnosis; the aggressiveness of osteosarcoma with rapid metastatic potential contributes to the poor prognosis of patients with the metastatic form of this disease (2,3). Multidrug regimens are used to control tumor cells at various stages of the cell cycle, eliminate local or distant micrometastases, and reduce the emergence of drug-resistant cells, which prolongs the overall and progression-free survival of patients with osteosarcoma compared with single-drug treatments, such as vincristine (VCR) (4,5). However, ≤40% of all human cancers develop multidrug resistance (MDR) following an initial period of response to treatment, and ~30% of osteosarcoma patients with MDR exhibit recurrence or metastasis during a five-year period (6-8). The mechanisms of drug resistance are multifactorial, including disruption of transporter pumps, oncogenes, tumor suppressor genes, DNA repair system, mitochondrial alterations, autophagy and epithelial-mesenchymal transition (9,10); however, the mechanisms underlying drug resistance are complex and require further investigation. Therefore, the associated molecular mechanisms and biomarkers should be identified.

The aim of the present study was to analyze the gene expression profiles of the human osteosarcoma cell line MG63 compared with VCR-resistant MG63 cells (MG63/VCR). These results may provide novel insight into identifying chemotherapeutic targets and developing more effective chemotherapy strategies for the treatment of osteosarcoma with VCR resistance.

Materials and methods

Cell culture. The human VCR-resistant osteosarcoma cell line MG63/VCR and its parental cell line MG63 were obtained from the Scientific Research Center, China-Japan Union Hospital of Jilin University (Jilin, China) (11). The cells were cultured in high-glucose Dulbecco's modified Eagle's medium (H-DMEM; Invitrogen, Thermo Fisher Scientific, Inc., Waltham, MA, USA) supplemented with 10% fetal bovine serum (FBS; HyClone; GE Healthcare Life Sciences, Logan, UT, USA) in a humidified atmosphere with 5% CO_2 at 37˚C; three biological replicates were conducted using the MG63 and MG63/VCR cells.

Cell viability assay. The cells were suspended at a density of $8x10^3$ cells per well and plated into 96-well plates in 100 μl H-DMEM supplemented with 10% FBS. Following incubation at 37˚C for 24 h, the cells were treated with VCR (New Hualian Pharmaceutical Co., Shanghai, China) at the following

Correspondence to: Professor Yan Wang, Science Research Center, China-Japan Union Hospital of Jilin University, 126 Xiantai Street, Changchun, Jilin 130033, P.R. China
E-mail: wangy01@jlu.edu.cn

Key words: osteosarcoma, drug resistance, microarray analysis

final concentrations: 2,000, 1,000, 500, 250, 125, and 62.5 ng/ml; drug-free medium was used as the control. MG63 cells were treated with the following concentrations: 64, 16, 4, 1, 0.25 and 0.0625 ng/ml. The half-maximal inhibitory concentration (IC_{50}) of VCR in MG63/VCR and MG63 cells was reported to be 453.4 and 0.952 ng/ml, respectively (11). A total of two groups of cells continued to culture 48 h in drug medium at 37˚C. Cell viability was examined using 10% Cell Counting kit-8 (CCK-8; Dojindo Molecular Technologies, Inc., Kumamoto, Japan) according to the manufacturer's protocols, and the cells were incubated at 37˚C for another 2 h. Subsequently, the optical density (OD) was determined by measuring the absorbance at 450 nm using a plate reader (UV8100D; LabTech, Inc., Hopkinton, MA, USA), and the inhibition ratio was calculated using the following formula: Inhibition ratio=$[(OD_{control}-OD_{experiment})/OD_{control}]$ x100%. Each experiment was performed in triplicate.

Total RNA extraction and microarray. Total RNA was extracted from the MG63/VCR and MG63 cells using TRIzol® reagent (Invitrogen; Thermo Fisher Scientific, Inc.). The quality of total RNA was determined using a NanoDrop 2000 spectrophotometer (1.7<A260/A280<2.2) and the RNA integrity (RIN) was evaluated using an Agilent Bioanalyzer 2100 (RIN≥7.0 and 28S/18S>0.7). The initial amount of total RNA (300-500 ng) was further amplified, labeled and purified by using the Microarray GeneChip 3'IVT Express kit (Affymetrix; Thermo Fisher Scientific, Inc.) According to the standard hybridization procedures and matching kit provided by Affymetrix expression chip. RNA was then subjected to treatment with the GeneChip Hybridization, Wash, and Stain kit reagent (Affymetrix; Thermo Fisher Scientific, Inc.), Rolling hybridization in a Hybridization Oven 645 for 45˚C, 16 h, and washed in GeneChip Fluidics Station 450 (Affymetrix; Thermo Fisher Scientific, Inc.) according to the manufacturer's protocols. The results of the chip were scanned with a GeneChip Scanner 3000 system (Affymetrix; Thermo Fisher Scientific, Inc.). Differentially expressed genes in the two cell lines were determined using the fold change (FC) values. The gene expression profile was presented in Excel spreadsheets (Microsoft Corporation, Redmond, WA, USA). Volcano plot, Scatter-plot and Clustergram were used to analyze the differential gene expression. Gene set enrichment analysis was performed using Ingenuity Pathway Analysis (IPA) online software (12,13).

Reverse transcription-quantitative polymerase chain reaction (RT-qPCR). Total RNA was extracted from the MG63/VCR and MG63 cells using TRIzol® reagent and reverse-transcribed into cDNA using RevertAid First Strand cDNA Synthesis kit (both Invitrogen; Thermo Fisher Scientific, Inc.) according to the manufacturer's protocols. The primers used for RT-qPCR were listed in Table I. qPCR was performed using SYBR® Premix Ex Taq™ II (Takara Biotechnology Co., Ltd., Dalian, China) on the Applied Biosystems 7500 Fast Real-Time PCR system (Applied Biosystems; Thermo Fisher Scientific, Inc.). The conditions used for qPCR were as follows: Denaturation at 95˚C for 30 sec; annealing at 58-62˚C for 30 sec; and 30 cycles of elongation at 95˚C for 15 sec, 60˚C for 30 sec, and 95˚C for 15 sec. The relative expression levels of each gene, normalized to the housekeeping gene *GAPDH*, was calculated using the $2^{-\Delta\Delta Cq}$ method (14).

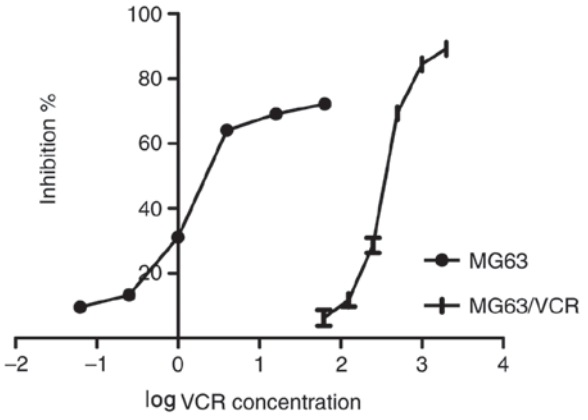

Figure 1. Effects of VCR on cell survival. The half-maximal inhibitory concentration at which VCR exhibited 50% inhibition on the viability of MG63 and MG63/VCR cells was determined with GraphPad Prism software using global nonlinear regression analysis. The X-axis represented log(VCR concentration), and the Y-axis indicated the inhibition ratio. VCR, vincristine.

Statistical analysis. Statistical analyses were performed using GraphPad Prism 5 (GraphPad Software, Inc., La Jolla, CA, USA), and all data are presented as the mean ± standard deviation. The statistical significance of the differences between the cell lines and treatments was analyzed by a Student's test or one-way analysis of variance and Tukey's test. IC_{50} was performed using global nonlinear regression analysis. Differential gene expression analysis was performed using a Student's t-test. The result of the chip analysis is the weighted average of repeated probe signals in each group. The threshold for statistical significance was P<0.05, |FC|>1.5. To systematically assign putative functions to the differentially expressed genes, bioinformatics analysis was performed with IPA. The unique statistical index of IPA is the z-score, which represents the direction and multiplier of the molecular changes under the existing experimental conditions. The z-score indicates whether the results are consistent with the references mentioned in the literature; inhibition or activation of the molecular action process was considered when |z|>2. A positive z-score suggests that the molecular interaction is activated, whereas a negative z-score indicates that the molecular interaction is inhibited.

Results

Sensitivity of MG63/VCR and MG63 cells to vincristine. To investigate the chemosensitivity of MG63/VCR and MG63 cells to VCR, the IC_{50} values in response to treatment with different VCR concentrations were determined. Following 48 h of culture in a VCR-containing medium, the IC50 value for MG63/VCR cells was significantly increased compared with that of MG63 cells (493.175±4.473 vs. 1.407±0.111 ng/ml, P=0.001), suggesting that MG63/VCR cells are more refractory to VCR compared with the parental MG63 cell line (Fig. 1).

Distinct gene expression landscapes between MG63/VCR and MG63 cells. In total, the genes that exhibited significantly aberrant expression between the two cell lines in

Table I. Primers used for reverse transcription-quantitative polymerase chain reaction.

Gene	Forward (5'-3')	Reverse (5'-3')
GAPDH	GCACCGTCAAGGCTGAGAAC	TGGTGAAGACGCCAGTGGA
MDR1	ATATCAGCAGCCCACATCAT	GAAGCACTGGGATGTCCGGT
IGF2BP1	CCACCAGTTGGAGAACCATGCC	ATGTCCACTTGCTGCTGCTTGG
TES	GCATGATGTCCTCTTGAGCAATGAAG	CATTCTTCTTGGCAGCAACTGGATTC
CAII	CTGAGCACTGGCATAAGGACTTCC	ATACTTGGCTGTATGAGTGTCGATGTC
AKAP12	CTCCACCGAGCAGCGCAG	GGTCCGAGGCAGCGATGG
COL1A2	TGTGATTTCTCTACTGGCGAAACC	ACGTGTTTCTTGTCCTTGGAGC
ROBO1	ACCCAGTAACTTGGCAGTAACTGT	TGGGCAGCTCTCCATCATCT
DAPK1	AGCACCGGCCTCCAGTATGC	TGTCCTCGCGGCTCACACC
SLIT2	TTAACTGTAACTGCTACCTGGCTTGG	TCATCACAAGTGAAGTCCTGAATGGC
FLRT3	GCTGTTCCTTCAAGTAGCACCTCTATC	TTGTAGCATCCTCTGGTATTCCTGTTG

MDR1, multi-drug resistance gene 1; IGF2BP1, insulin-like growth factor-II binding protein 1; TES, testin LIM domain protein; CAII, carbonic anhydrase II; AKAP12, A-kinase anchor protein 12; COL1A2, collagen A2; ROBO1, roundabout homolog 1; DAPK1, death-associated protein kinase 1; SLIT2, slit guidance ligand 2; FLRT3, fibronectin leucine rich transmembrane protein 3.

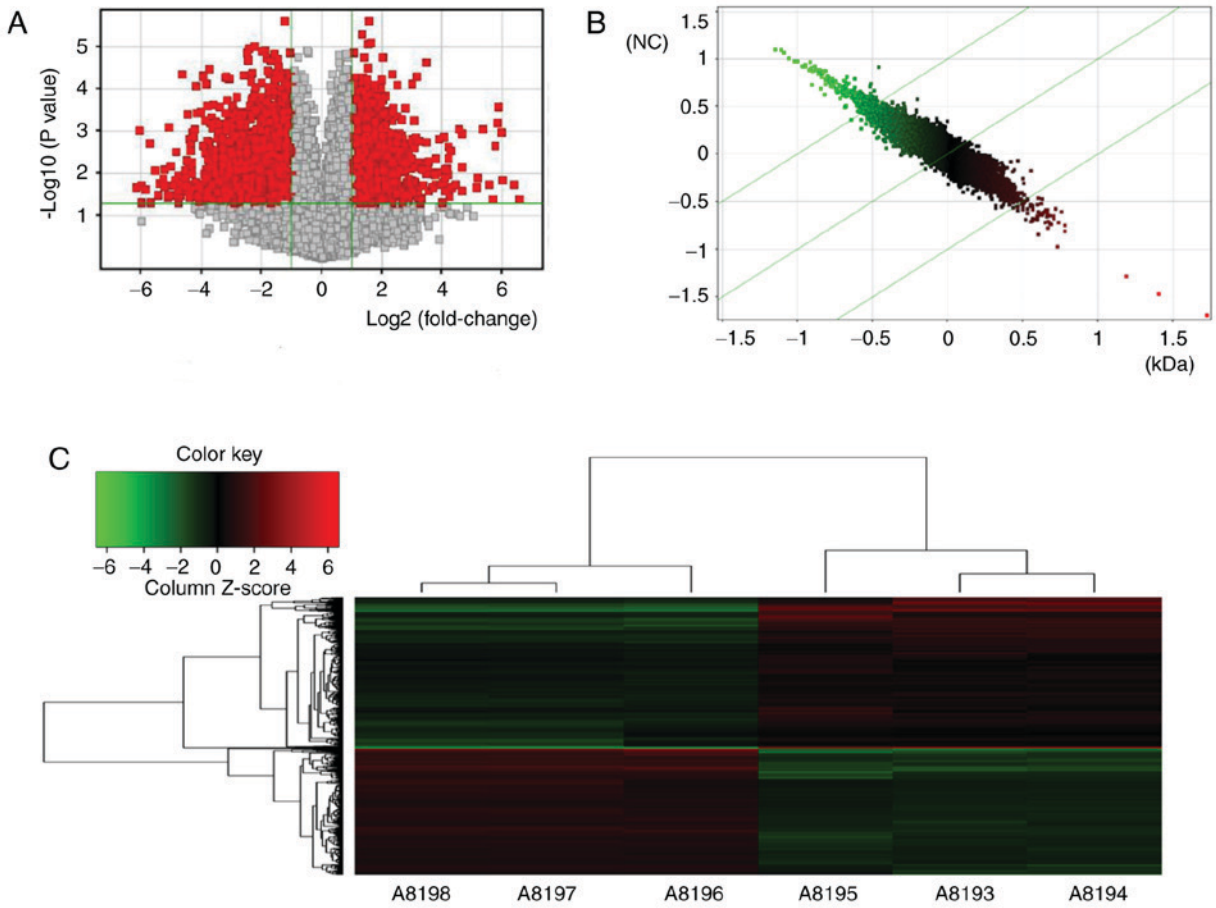

Figure 2. Differentially expressed genes in MG63/VCR and MG63 cells based on microarray analysis. (A) Volcano plot: The X-axis represented the fold change values (log_2-scaled), and the Y-axis indicated the corrected P-values (log_{10}-scaled); the red dots represented differentially expressed genes with statistical significance. (B) Scatter-plot: The X-axis represented the data of the control group and the Y-axis indicated the data of the experimental groups. The data above or below the highest green line indicated that the probe was downregulated or upregulated, respectively, in MG63/VCR cells compared with MG63 cells. (C) Clustergram: Each row and column represented a gene and sample, respectively. A8193, A8194 and A8195 represented the three samples of MG63 cells; A8196, A8197 and A8198 represented the three samples of MG63/VCR cells. Red indicates upregulated gene expression and green indicates downregulated gene expression.

microarray analysis were evaluated by volcano plot filtering (P<0.05, FC≥1.5; Fig. 2A). A total of 602 genes were upregulated and 698 were downregulated in MG63/VCR cells compared with MG63 cells. The scatterplot and cluster

Table II. Genes with downregulated expression in MG63/VCR relative to MG63 cells.

Gene	Gene name	P-value	Fold change	False discovery rate
Transcription factors				
TP63	Tumor protein 63	0.00092	-7.26360	0.00266
ZEB2	Zinc finger E-box binding homeobox 2	0.00016	-4.23951	0.00145
Transporters				
FABP5	Fatty acid binding protein 5 (psoriasis-associated)	<0.00001	-66.32220	0.00035
ABCA8	ATP-binding cassette, sub-family A (ABC1), member 8	0.00055	-4.11858	0.00220
Transmembrane receptors				
IL13RA2	Interleukin 13 receptor, a2	0.00008	-15.08010	0.00111
Enzymes				
PLSCR4	Phospholipase scramblase 2	0.00226	-5.89258	0.00442
CHI3L1	Chitinase 3-like 1 (cartilage glycoprotein-39)	<0.00001	-196.98900	0.00061
TGM2	Transglutaminase 2	0.00006	-4.85356	0.00106
EFEMP1	EGF containing fibulin-like extracellular matrix protein 1	0.00011	-5.37078	0.00124
MSMO1	Methylsterol monooxygenase 1	0.00232	-8.35006	0.00449
LOX	Lysyl oxidase	0.00035	-4.77463	0.00180
AKR1C3	Aldo-keto reductase family 1, member C3	0.00009	-6.83914	0.00116
Other				
IL15	Interleukin 15	0.00427	-4.77006	0.00698
CCL2	Chemokine (C-C motif) ligand 2	0.00107	-7.26246	0.00288
KCNK2	Potassium channel, two pore domain subfamily K, member 2	0.00017	-5.20959	0.00146
KCNJ2	Potassium channel, inwardly rectifying subfamily J, member 2	0.00017	-4.15907	0.00146
DAPK1	Death-associated protein kinase 1	0.00072	-5.37922	0.00242
DKK1	Dickkopf WNT signaling pathway inhibitor 1	0.00007	-6.61779	0.00109
GSAP	γ-secretase activating protein	0.00104	-4.12709	0.00283
ADAMTS1	ADAM metallopeptidase with thrombospondin type 1 motif, 1	<0.00001	-4.76113	0.00058
SLIT2	Slit guidance ligand 2	0.00037	-8.33081	0.00186
THBS2	Thrombospondin 2	<0.00001	-4.12890	0.00047
CCDC102B	Coiled-coil domain containing 102B	0.00063	-6.34919	0.00230
CDH2	Cadherin 2, type 1, N-cadherin (neuronal)	<0.00001	-8.36960	0.00045
TM4SF18	Transmembrane 4 L six family member 18	0.00016	-6.42868	0.00145
FLRT3	Fibronectin leucine rich transmembrane protein 3	0.00057	-5.87903	0.00224
THY1	Thy-1 cell surface antigen	<0.00001	-18.64350	0.00046
SHISA3	Shisa family member 3	<0.00001	-8.51613	0.00035
ITGB8	Integrin, b8	0.00578	-4.32276	0.00873
CDH11	Cadherin 11, type 2, OB-cadherin (osteoblast)	0.00001	-8.02862	0.00065
COL3A1	Collagen, type III, a1	0.00011	-11.94630	0.00124
PCDH18	Protocadherin 18	0.00109	-4.42683	0.00290
LRCH2	Leucine-rich repeats and calponin homology (CH) domain containing 2	0.00129	-5.18966	0.00321
SEMA6D	Sema domain, transmembrane domain (TM), and cytoplasmic domain, (semaphorin) 6D	0.00004	-4.88122	0.00096
TES	Testin LIM domain protein	0.00015	-22.05530	0.00139
LUM	Lumican	0.00582	-4.02085	0.00877
SPRY1	Sprouty RTK signaling antagonist 1	0.00009	-6.06186	0.00116

Table II. Continued.

Gene	Gene name	P-value	Fold change	False discovery rate
Other				
CD46	CD46 molecule, complement regulatory protein	0.01614	-4.36522	0.01969
CCNG1	Cyclin G1	0.00188	-6.89583	0.00396
ABI3BP	ABI family, member 3 (NESH) binding protein	0.00005	-6.61567	0.00106
FLRT2	Fibronectin leucine rich transmembrane protein 2	0.00004	-4.43384	0.00098
SNTB1	Syntrophin, b1 (dystrophin-associated protein A1, 59kDa, basic component 1)	0.00068	-4.41392	0.00236
AIF1L	Allograft inflammatory factor 1-like	0.00014	-8.21928	0.00138
GAL	Galanin/GMAP prepropeptide	<0.00001	-11.35750	0.00051
VCAN	Versican	0.00019	-12.17840	0.00152

analysis (Fig. 2B and C) revealed the differential expression profiles of the genes.

Evaluation of the diagnostic potential of differentially expressed genes. To evaluate the diagnostic potential of differentially expressed genes in VCR-resistant MG63 cells, 45 of the downregulated genes (Table II) and 26 of the upregulated genes (Table III) with statistical significance at P<0.05 and a ≥4-fold difference in expression levels between the two cell lines, were selected for further analysis. Based on their putative functions, all genes (Tables II and III) were categorized into subgroups, including transcription factors (n=2+2), enzymes (n=7+5), transporters (n=2+3), transmembrane receptors (n=1+3) and others (n=33+13).

Signaling pathways analysis. To systematically assign putative functions to the differentially expressed genes, bioinformatics analysis was performed. Among the 800 signaling pathways identified by IPA, the major signaling pathways regulated by the differentially expressed genes were enriched in B-cell receptor signaling [including early growth response protein 1, mitogen-activated protein kinases 9 (MAPK9), cell division control protein 42 homolog and protein phosphatase 3 catalytic subunit A], ultraviolet A (UVA)-induced MAPK signaling [including phosphoinositide-3-kinase regulatory subunit 1, MAPK9 and epidermal growth factor receptor (EGFR)] and Erb-B2 receptor tyrosine kinase 2/3 (ErbB2/3) signaling pathways (including RAS related 2, signal transducer and activator of transcription 5B and serine/threonine kinase ATM; Table IV). The first two pathways were predicted to be inhibited, while the last pathway was predicted to be promoted by VCR, suggesting that combination therapy with EGFR inhibitor and VCR may be more effective compared with single-drug therapy. The top enriched pathway was UVA-induced MAPK signaling (Fig. 3A and B), with a z-score of -2.309. The data, together with the predicted signaling pathways, may provide novel insight in determining whether the aberrant expression of these molecules, such as EGFR, may contribute to drug resistance.

RT-qPCR validation of differentially expressed genes. A total of 10 of the differentially expressed genes identified by microarray analysis were selected for further validation using RT-qPCR, including six upregulated genes [multi-drug resistance gene1 (*MDR1*), carbonic anhydrase II (*CAII*), insulin-like growth factor-II binding protein 1 (*IGF2BP1*), A-kinase anchor protein 12 (*AKAP12*), roundabout homolog 1 (*ROBO1*) and collagen A2 (*COL1A2*)], and four downregulated genes, including slit guidance ligand 2, death-associated protein kinase 1 (*DAPK1*), fibronectin leucine rich transmembrane protein 3 (*FLRT3*) and testin LIM domain protein. As presented in Fig. 4, the expression profiles of the 10 genes were consistent with the microarray data; however, the FC values varied to an extent. RT-qPCR revealed that the expression levels of FLRT3 were increased in MG63/VCR cells, which is in controversy with the microarray data. Thus, 9 of the 10 genes were positively determined by RT-qPCR.

Discussion

Personalized chemotherapy based on biomarkers may improve the sensitivity to chemotherapy and the clinical outcome of patients with cancer. Thus, investigating the molecular mechanisms underlying drug resistance is essential to develop a personalized chemotherapy regimen and prevent drug resistance during cancer therapy. In the present study, the roles of differentially expressed genes in VCR resistance of osteosarcoma cells were investigated by microarray analysis. Numerous genes determined as differentially expressed in VCR-resistant osteosarcoma cells may also be associated with VCR resistance in the present study, such as *MDR1* (11), which was upregulated in MG63/VCR cells. Previous studies have indicated that *MDR1*serves a key role in the proliferation and survival of epithelial and malignant cells during tumorigenesis, as well as in acquired drug resistance (15,16). Few of the differentially expressed genes identified in the present study, including *CAII* and *IGF2BP1*, have also been reported to promote cell invasion and drug resistance (17,18); however, some results were in conflict with previous studies. For example, zinc finger E-box binding homeobox 2and chitinase

Table III. Genes with upregulated expression of MG63/VCR relative to MG63 cells.

Gene symbol	Gene name	P-value	Fold change	False discovery rate
Transcriptional regulators				
RBPMS	RNA-binding protein with multiple splicing	0.00017	4.21538	0.00147
HEY1	Hes-related family bHLH transcription factor with YRPW motif 1	0.00140	4.53673	0.00336
Transporters				
BET1	Bet1 Golgi vesicular membrane trafficking protein	0.00009	5.03427	0.00117
AKAP12	A kinase (PRKA) anchor protein 12	0.00011	4.74115	0.00124
MDR1	ATP-binding cassette, sub-family B (MDR/TAP), member 1	<0.00001	50.25262	0.00036
Transmembrane receptors				
F3	Coagulation factor III (thromboplastin, tissue factor)	0.00368	6.49217	0.00621
TNFRSF19	Tumor necrosis factor receptor superfamily, member 19	0.00037	7.31358	0.00185
ROBO1	Roundabout guidance receptor 1	<0.00001	6.28868	0.00035
Enzymes				
GNG11	Guanine nucleotide binding protein (G protein) g11	0.00001	4.43954	0.00065
RNF182	Ring finger protein 182	<0.00001	9.08702	0.00036
OTUB2	OTU deubiquitinase, ubiquitin aldehyde binding 2	0.00200	4.41107	0.00410
EPHX4	Epoxide hydrolase 4	0.00024	4.63712	0.00160
CA2	carbonic anhydrase II	<0.00001	10.07676	0.00022
Others				
IGF2BP1	Insulin-like growth factor 2 mRNA-binding protein I	<0.00001	10.19015	0.00051
KIAA1324L	KIAA1324-like	0.00039	4.86219	0.00192
PTPRQ	protein tyrosine phosphatase, receptor type, Q	0.00256	7.63223	0.00479
FAM101B	family with sequence similarity 101, member B	0.00176	4.34868	0.00382
TNNT1	Troponin T type 1 (skeletal, slow)	0.00070	4.17861	0.00241
COL1A2	Collagen, type I, a2	0.00173	5.21119	0.00377
ESRP1	Epithelial splicing regulatory protein 1	0.01391	8.18397	0.01748
RBM48	RNA binding motif protein 48	0.00151	4.44897	0.00352
KLHL13	Kelch-like family member 13	0.00022	4.27967	0.00156
DSP	Desmoplakin	0.00002	7.71674	0.00077
NEFL	Neurofilament, light polypeptide	0.00048	4.07517	0.00208
AMIGO2	Adhesion molecule with Ig-like domain 2	0.01035	4.29618	0.01381
AKAP9	A kinase (PRKA) anchor protein 9	0.00038	7.09333	0.00189

3-like 1 (cartilage glycoprotein-39) were downregulated in MG63/VCR cells compared with MG63 cells, which is inconsistent with other studies (19,20); this may be caused by experimental errors. Different experimental conditions, including sample types, processing methods and sampling time may result in differences in gene expression, which may also be affected by a variety of factors, such as PCR conditions and chip analysis. In addition, there is a lack of data to effectively predict the functions of some of the aberrantly expressed genes at present, including *AKAP12*, *DAPK1* and *ROBO1*, which may be the potential genes associated with drug resistance; however, further investigation is required.

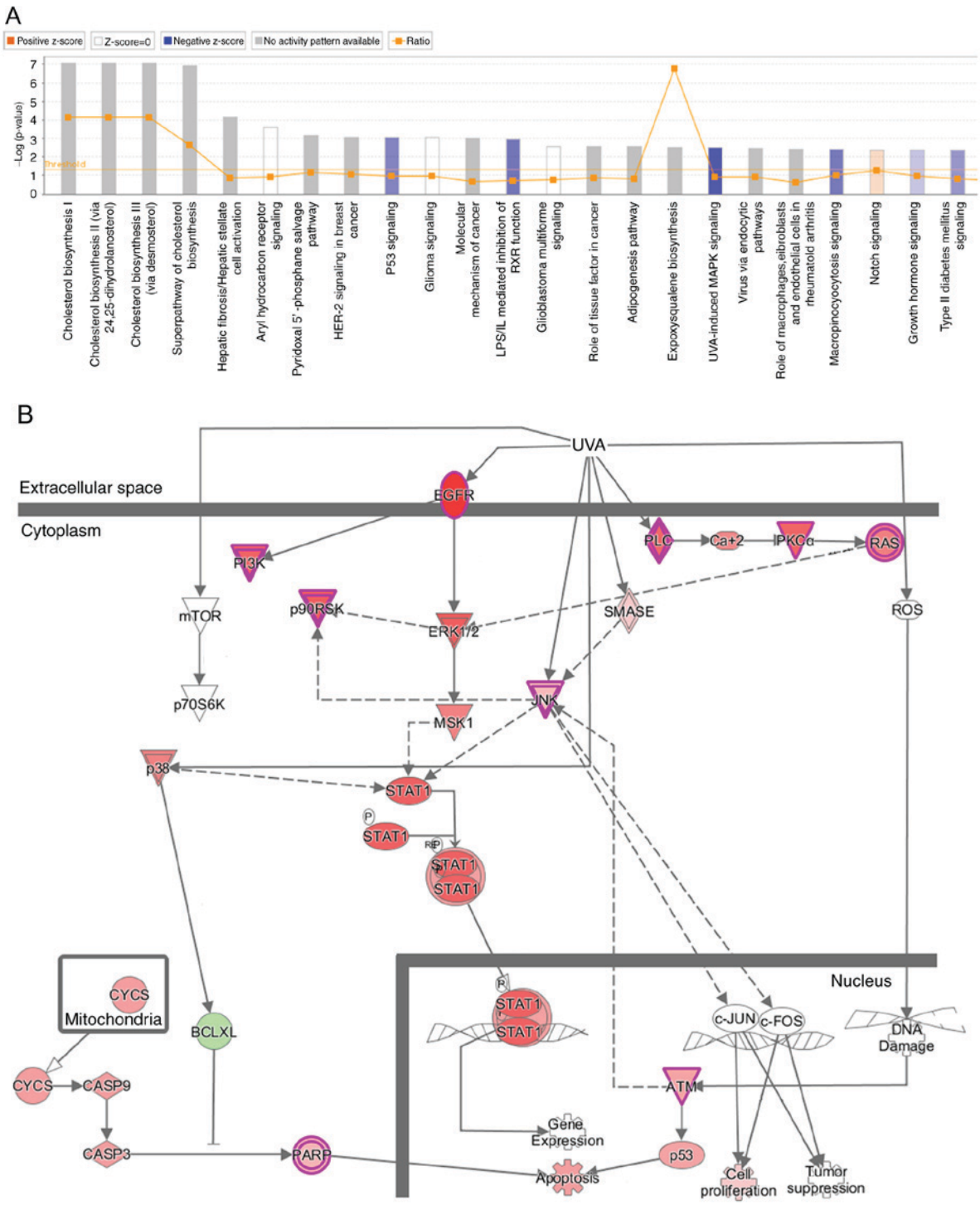

Figure 3. Signaling pathways regulated by differentially expressed genes. (A) Histogram represented enrichment analysis of signaling pathways regulated by differentially expressed genes, ranked by the log P-value; orange indicates z>0 and blue indicates z<0. The ratio revealed the number of differentially expressed genes among all the genes involved in the signaling pathways. (B) UVA-induced mitogen-activated protein kinase signaling. Red indicated upregulation; green indicated downregulation; higher intensity presented predicted activation with higher confidence than lower intensity; solid line, direct interaction; dotted line, indirect interaction; UVA, ultraviolet A.

IPA analysis can aid the investigation of novel molecular mechanisms underlying drug resistance. For example, a previous study revealed that the expression levels of *COL1A2* and insulin like growth factor 1 receptor (*IGF1R*), along with the associated pathways, were induced in ovarian cancer cells with topotecan- and paclitaxel-resistance (21). In addition, IGF1R-induced chemoresistance of tumor cells was associated with the signaling pathways involved in the promotion of cell proliferation, inhibition of apoptosis, regulation of ATP-binding cassette transporter proteins and interactions with the extracellular matrix (22); however, other mechanisms underlying drug resistance require further investigation.

Furthermore, signaling pathway analysis revealed that differently expressed genes are mainly enriched in pathways,

Table IV. Canonical pathways for gene enrichment of differentially expressed genes in MG63/VCR relative to MG63 cells.

Canonical Pathways	-log(P-value)	Ratio	z-score	Molecules
UVA-induced MAPK signaling	2.51	0.136	-2.309	PLCE1, RRAS2, PIK3R1, ZC3HAV1, MAPK9, TNKS2, PLCL2, RPS6KA1, PARP14, PRKCA, ATM, EGFR
Role of NFAT in cardiac hypertrophy	2.33	0.106	-2.065	IL6ST, PIK3R1, MAPK9, PLCL2, HDAC6, CAMK2D, GNG11, PLCE1, RRAS2, MEF2D, PPP3R1, IGF1R, PRKAG2, PRKCE, MEF2C, SLC8A1, PPP3CA, ATM, PRKCA
LPS-stimulated MAPK signaling	1.74	0.123	-2.121	RRAS2, CDC42, PIK3R1, PRKCE, CD14, MAPK9, MAP3K5, PRKCA, ATM
14-3-3-mediated signaling	1.56	0.103	-2.530	SRPK2, PLCE1, RRAS2, PIK3R1, PRKCE, MAPK9, PLCL2, BAX, MAP3K5, RPS6KA1, PRKCA, ATM
B cell receptor signaling	1.24	0.086	-3.207	RAP2A, PIK3R1, EGR1, MAPK9, INPPL1, MALT1, MAP3K5, EBF1, CAMK2D, RRAS2, CDC42, PPP3R1, MEF2C, PPP3CA, ATM
HGF signaling	1.20	0.095	-2.530	RRAS2, CDC42, PIK3R1, CDKN1A, PRKCE, MAPK9, MAP3K5, ITGA4, PRKCA, ATM
Role of pattern recognition receptors in recognition of bacteria and viruses	1.08	0.088	-2.333	PTX3, IL18, C3, PIK3R1, DDX58, CASP1, PRKCE, MAPK9, EIF2AK2, PRKCA, ATM
mTOR signaling	1.03	0.080	-2.138	NAPEPLD, ULK1, DDIT4, PIK3R1, FKBP1A, EIF4E, RRAS2, IRS1, PRKAG2, PRKAA1, PRKCE, RPS6KA1, ATM, RPS14, PRKCA
Endothelin-1 signaling	1.03	0.081	-2.111	NAPEPLD, PIK3R1, MAPK9, PLCL2, RRAS2, PLCE1, GNAO1, CASP1, RARRES3, PRKCE, ECE1, CASP7, ATM, PRKCA
Signaling by Rho family GTPases	1.02	0.077	-2.000	PIK3R1, WASF3, CDH6, MAPK9, MYLK, CDH11, LIMK1, CDH2, ARPC1A, GNG11, CDH5, CDC42, EZR, GNAO1, ARHGEF18, ARHGEF9, ATM, ITGA4
HMGB1 signaling	0.90	0.083	-2.530	IL18, ICAM1, RRAS2, CCL2, CDC42, PIK3R1, MAPK9, TNFRSF11B, ATM, PLAT
Leukocyte extravasation signaling	0.88	0.076	-2.111	ICAM1, PIK3R1, THY1, MAPK9, MLLT4, CDH5, CDC42, JAM3, EZR, CD44, PRKCE, ATM, PRKCA, ITGA4, CTNND1
CNTF signaling	0.81	0.096	-2.236	IL6ST, RRAS2, PIK3R1, RPS6KA1, ATM
Role of NANOG in mammalian embryonic stem cell pluripotency	0.80	0.081	-2.000	IL6ST, RRAS2, WNT3, PIK3R1, WNT2B, SMAD4, FZD1, BMP5, ATM
FcγRIIB signaling in B lymphocytes	0.73	0.098	-2.000	RRAS2, PIK3R1, MAPK9, ATM
NGF signaling	0.63	0.075	-2.828	RRAS2, CDC42, PIK3R1, MAPK9, BAX, MAP3K5, RPS6KA1, ATM
CD28 signaling in T helper cells	0.49	0.068	-2.828	ARPC1A, CDC42, PIK3R1, PPP3R1, MAPK9, MALT1, PPP3CA, ATM
RANK signaling in osteoclasts	0.45	0.068	-2.449	PIK3R1, PPP3R1, MAPK9, MAP3K5, PPP3CA, ATM
ErbB2-ErbB3 signaling	0.42	0.070	2.000	RRAS2, PIK3R1, STAT5B, ATM
Insulin receptor signaling	0.36	0.061	-2.121	RRAS2, IRS1, PIK3R1, PRKAG2, IRS2, INPPL1, EIF4E, ATM
Renal cell carcinoma signaling	0.26	0.056	-2.000	RRAS2, CDC42, PIK3R1, ATM

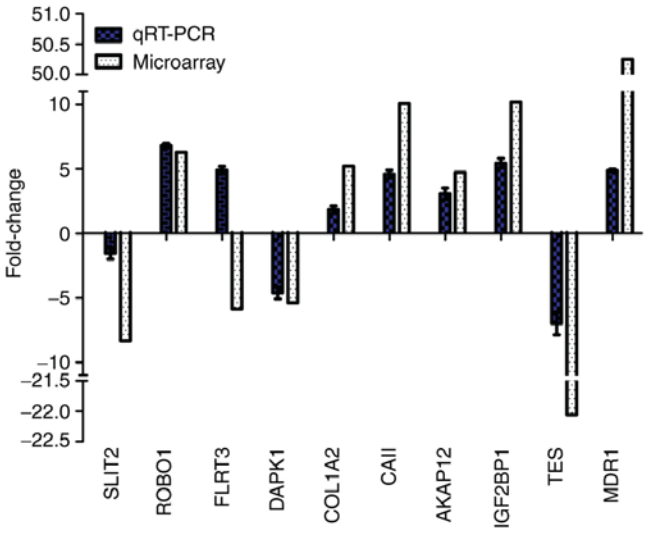

Figure 4. RT-qPCR validation of the microarray results for ten selected genes. Relative fold changes as determined by RT-qPCR are plotted against the microarray data. AKAP12, A-kinase anchor protein 12; CAII, carbonic anhydrase II; COL1A2, collagen A2; DAPK1, death-associated protein kinase 1; FLRT3, fibronectin leucine rich transmembrane protein 3; IGF2BP1, insulin-like growth factor-II binding protein 1; MDR1, multi-drug resistance gene1; ROBO1, roundabout homolog 1; RT-qPCR, reverse transcription-quantitative polymerase chain reaction; SLIT2, slit guidance ligand 2; TES, testin LIM domain protein.

including B cell receptor signaling, UVA-induced MAPK signaling and ErbB2-ErbB3 signaling, which were previously associated with drug resistance (23-25). For instance, B-cell receptor signaling was reported as an essential mediator of cytoskeletal reorganization, integrin clustering and environmental-mediated drug resistance (23). A recent study revealed that the steroidal lactone withaferin A may serve as a low-toxicity addition to ERBB2-targeted therapeutics, particularly when ERBB3 induced resistance or reduced overall sensitivity (24). Several studies have indicated that numerous proteins are involved in UVA-induced MAPK signaling, such as EGFR (P=0.003473, FC=1.95397), which was upregulated in MG63/VCR cells and maybe a key regulator in the pathways associated with VCR resistance (25,26). EGFR is a transmembrane tyrosine kinase receptor, and is one of the most extensively studied MDR-associated receptors (25). Inhibition of the EGFR/HER2 signaling pathway, particularly the activity of downstream PI3K, induced a more favorable milieu for tumor immunotherapy (26). While the UVA-induced MAPK signaling pathway was downregulated in MG63-VCR cells, EGFR was upregulated; however, the effects of this pathway on drug resistance remain unknown.

In conclusion, differentially expressed genes were identified between MG63/VCR and MG63 cells in the present study. These results revealed the potential functions of these genes, providing novel insight into their roles in drug resistance and associated pathways, which may aid the identification of novel potential targets for the treatment of osteosarcoma.

Acknowledgements

Not applicable.

Funding

The present study was supported by the International Cooperation of Jilin Provincial Science & Technology Department (grant no. 20150101175JC) and the National Natural Science Foundation of China (grant nos. 81172000 and 30772488).

Availability of data and materials

The datasets used or analysed during the current study are available from the corresponding author on reasonable request.

Authors' contributions

YW was the person in charge of this project, responsible for overall planning and specific project implementation. YW and RC conceived and designed the study. L-HH has provided technical support and experimental guidance in the construction of multidrug resistant cell sublines and is responsible for monitoring the stability of multidrug resistant cells. RC, Y-YG, J-ZY performed the experiments. YW and RC wrote the paper. RC, Y-YG, J-ZY, L-HH and YW reviewed and edited the manuscript. All authors read and approved the manuscript.

Ethics approval and consent to participate

Not applicable.

Patient consent for publication

Not applicable.

Competing interests

The authors declare that they have no competing interests.

References

1. Cai S, Zhang T, Zhang D, Qiu G and Liu Y: Volume-sensitive chloride channels are involved in cisplatin treatment of osteosarcoma. Mol Med Rep 11: 2465-2470, 2015.
2. Zhang Y, Zhang L, Zhang G, Li S, Duan J, Cheng J, Ding G, Zhou C, Zhang J, Luo P, *et al*: Osteosarcoma metastasis: Prospective role of ezrin. Tumor Biol 35: 5055-5059, 2014.
3. Luetke A, Meyers PA, Lewis I and Juergens H: Osteosarcoma treatment-where do we stand? A state of the art review. Cancer Treat Rev 40: 523-532, 2014.
4. Wang Y and Teng JS: Increased multi-drug resistance and reduced apoptosis in osteosarcoma side population cells are crucial factors for tumor recurrence. Exp Ther Med 12: 81-86, 2016.
5. Wang X, Zheng H, Shou T, Tang C, Miao K and Wang P: Effectiveness of multi-drug regimen chemotherapy treatment in osteosarcoma patients: A network meta-analysis of randomized controlled trials. J Orthop Surg Res 12: 52, 2017.
6. Hattinger CM, Pasello M, Ferrari S, Picci P and Serra M: Emerging drugs for high-grade osteosarcoma. Expert Opin Emerg Drugs 15: 615-634, 2010.
7. Chou AJ and Gorlick R: Chemotherapy resistance in osteosarcoma: Current challenges and future directions. Expert Rev Anticancer Ther 6: 1075-1085, 2016.
8. Ottaviani G and Jaffe N: The epidemiology of osteosarcoma. Cancer Treat Res 152: 3-13, 2009.
9. Brasseur K, Gévry N and Asselin E: Chemoresistance and targeted therapies in ovarian and endometrial cancers. Oncotarget 8: 4008-4042, 2017.

10. Lu C and Shervington A: Chemoresistance in gliomas. Mol Cell Biochem 312: 71-80, 2008.
11. Yang JZ, Ma SR, Rong XL, Zhu MJ, Ji QY, Meng LJ, Gao YY, Yang YD and Wang Y: Characterization of multidrug-resistant osteosarcoma sublines and the molecular mechanisms of resistance. Mol Med Rep 14: 3269-3276, 2016.
12. Felciano RM, Bavari S, Richards DR, Billaud JN, Warren T, Panchal R and Krämer A: Predictive systems biology approach to broad-spectrum, host-directed drug target discovery in infectious diseases. Pac Symp Biocomput: 17-28, 2013.
13. Calvano SE, Xiao W, Richards DR, Felciano RM, Baker HV, Cho RJ, Chen RO, Brownstein BH, Cobb JP, Tschoeke SK, *et al*: A network-based analysis of systemic inflammation in humans. Nature 437: 1032-1037, 2013.
14. Livak KJ and Schmittgen TD: Analysis of relative gene expression data using real-time quantitative PCR and the 2(-Delta Delta C(T)) method. Methods 25: 402-408, 2001.
15. Wang Z, Xia Q, Cui J, Diao Y and Li J: Reversion of P-glycoprotein-mediated multidrug resistance by diallyl trisulfide in a human osteosarcoma cell line. Oncol Rep 31: 2720-2726, 2014.
16. Tahara T, Arisawa T, Shibata T, Hirata I and Nakano H: Multi-drug resistance 1 polymorphism is associated with reduced risk of gastric cancer in the Japanese population. J Gastroenterol Hepatol 22: 1678-1682, 2007.
17. Zhou R, Huang W, Yao Y, Wang Y, Li Z, Shao B, Zhong J, Tang M, Liang S, Zhao X, *et al*: CA II, a potential biomarker by proteomic analysis, exerts significant inhibitory effect on the growth of colorectal cancer cells. Int J Oncol 43: 611-621, 2013.
18. Faye MD, Beug ST, Graber TE, Earl N, Xiang X, Wild B, Langlois S, Michaud J, Cowan KN, Korneluk RG and Holcik M: IGF2BP1 controls cell death and drug resistance in rhabdomyosarcomas by regulating translation of cIAP1. Oncogene 34: 1532-1541, 2015.
19. Xie XQ, Zhao QH, Wang H and Gu KS: Dysregulation of mRNA profile in cisplatin-resistant gastric cancer cell line SGC7901. World J Gastroentero 23: 1189-1202, 2017.
20. Chiang YC, Lin HW, Chang CF, Chang MC, Fu CF, Chen TC, Hsieh SF, Chen CA and Cheng WF: Overexpression of CHI3L1 is associated with chemoresistance and poor outcome of epithelial ovarian carcinoma. Oncotarget 6: 39740-39755, 2015.
21. Januchowski R, Świerczewska M, Sterzyńska K, Wojtowicz K, Nowicki M and Zabel M: Increased expression of several collagen genes is associated with drug resistance in ovarian cancer cell lines. J Cancer 7: 1295-1310, 2016.
22. Yuan J, Yin Z, Tao K, Wang G and Gao J: Function of insulin-like growth factor 1 receptor in cancer resistance to chemotherapy. Oncol Lett 15: 41-47, 2018.
23. Spaargaren M, Beuling EA, Rurup ML, Meijer HP, Klok MD, Middendorp S, Hendriks RW and Pals ST: The B cell antigen receptor controls integrin activity through Btk and PLCgamma2. J Exp Med 198: 1539-1550, 2003.
24. Liu W, Barnette AR, Andreansky S and Landgraf R: ERBB2 overexpression establishes ERBB3-dependent hypersensitivity of breast cancer cells to withaferin A. Mol Cancer Ther 15: 2750-2757, 2016.
25. Ekstrand AJ, James CD, Cavenee WK, Seliger B, Pettersson RF and Collins VP: Genes for epidermal growth factor receptor, transforming growth factor, and epidermal growth factor and their expression in human gliomas in vivo. Cancer Res 51: 2164-2172, 1991.
26. Suh KJ, Sung JH, Kim JW, Han SH, Lee HS, Min A, Kang MH, Kim JE, Kim JW, Kim SH, *et al*: EGFR or HER2 inhibition modulates the tumor microenvironment by suppression of PD-L1 and cytokines release. Oncotarget 8: 63901-63910, 2017.